

Observation of Spin Flips with a Single Trapped Proton

S. Ulmer^{1,2,3}, C.C. Rodegheri^{1,2}, K. Blaum^{1,3}, H. Kracke^{2,4}, A. Mooser^{2,4}, W. Quint^{3,5}, J. Walz^{2,4}

¹ *Max-Planck-Institut für Kernphysik, Saupfercheckweg 1, D-69117 Heidelberg, Germany*

² *Institut für Physik, Johannes Gutenberg-Universität D-55099 Mainz, Germany*

³ *Ruprecht Karls-Universität Heidelberg, D-69047 Heidelberg, Germany*

⁴ *Helmholtz Institut Mainz, D-55099 Mainz, Germany and*

⁵ *GSI - Helmholtzzentrum für Schwerionenforschung, D-64291 Darmstadt, Germany*

(Dated: December 31, 2018)

Spin transitions of an isolated trapped proton are observed for the first time. The spin quantum jumps are detected via the continuous Stern-Gerlach effect which is used in an experiment with a single proton stored in a cryogenic Penning trap. This opens the way for a direct high-precision measurement of the magnetic moment of the proton and a new test of the matter-antimatter symmetry in the baryon sector. This method can also be applied to other light atomic nuclei.

PACS numbers: 14.20.Dh 21.10.Ky 37.10.Dy

The challenge to understand the structure of the proton and to measure its properties inspires very different branches of physics. A global programme in high-energy spin physics is dedicated to the spin structure of the proton which is one of the most challenging open puzzles in quantum chromodynamics [1]. In atomic physics, on the other hand, some important precision experiments are plagued by a lack of knowledge about proton structure. The precision with which quantum electrodynamics can be tested by ultrahigh-resolution laser spectroscopy of hydrogen used to be limited by the precision with which the proton radius is known [2]. The argument can be turned around, of course, and precision atomic physics can be used to establish constraints on proton structure [3]. Spectacular progress has been made very recently in an experiment which used laser spectroscopy of muonic hydrogen to determine the radius of the proton [4].

Another important property of the proton is its magnetic moment $\mu_p = (g_p/2)\mu_N$, where g_p is the Landé g -factor, $\mu_N = e\hbar/(2m_p)$ is the nuclear magneton, and e/m_p is the charge-to-mass ratio. The most precise value for $g_p = 5.585\,694\,706(56)$ is extracted [5] from a measurement of the ground-state hyperfine splitting in hydrogen about forty years ago [6]. The hyperfine splitting itself is known with very high precision to 6 parts in 10^{13} [7]. However, the electron wave function overlaps with the proton. Hyperfine splitting is thus sensitive to proton form factors [3] and the precision of the proton g -factor is 1 part in 10^8 , only [5].

Our experiment aims at measuring the magnetic moment of the proton directly [8, 9] and does not require any theoretical correction. The experiment uses just one single isolated particle. Unlike in hyperfine splitting, there is no electron involved. Thus the experiment is “clean” in the sense that proton size and proton structure do not enter. It should be possible to improve the accuracy of the proton g -factor by one order of magnitude, at least. In addition, an independent measurement of the magnetic moment of the proton might be useful in combi-

nation with the hyperfine splitting to derive additional constraints on proton structure.

The same techniques can also be used to measure the magnetic moment of the antiproton, which presently is known at a level of 10^{-3} , only [10, 11]. Thus, an improvement by six orders of magnitude is possible, which will represent a stringent test of the matter-antimatter symmetry (CPT -symmetry) in the baryon sector [12].

The experiment is based on the continuous Stern-Gerlach effect in Penning traps [13]. This elegant scheme for the non-destructive determination of the spin direction has been used with great success in measurements of the g -factor of the electron [14], the positron [15] and of bound electrons [16, 17]. All these experiments dealt with magnetic moments on the level of the *Bohr magneton*. A measurement of the magnetic moment of the proton is much more challenging, because it is on the level of the *nuclear magneton*, which is three orders of magnitude smaller.

In this Letter we demonstrate the detection of spin flips of a single proton stored in a Penning trap which is the most important break-through for our experiment.

A double Penning trap [8] consisting of a precision trap

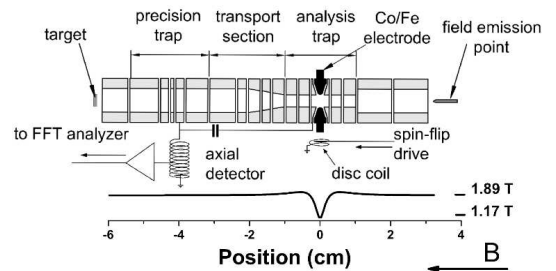


FIG. 1. Schematic of the proton g -factor experiment. The system consists of two Penning traps which are connected by transport electrodes. The central ring electrode of the analysis trap is made of ferromagnetic material. The lower graph shows the magnitude of the magnetic field along the axis. For further details see text.

(PT) and an analysis trap (AT) is mounted in the horizontal bore of a superconducting magnet with a magnetic field of 1.89 T. Both traps are of cylindrical and compensated design [18]. The precision trap has an inner radius of 3.5 mm and is located in the homogeneous center of the magnetic field. The ring electrode of the analysis trap has an inner radius of 1.8 mm and is made out of ferromagnetic Co/Fe-material which distorts the homogeneous magnetic field. Near the center of the trap the magnetic field is approximately described by

$$\vec{B} = B_0 \vec{e}_z + B_2 ((z^2 - \rho^2/2) \vec{e}_z - z \rho \vec{e}_\rho) . \quad (1)$$

The “magnetic bottle” coefficient $B_2 = 3.00(10) \cdot 10^5 \text{ T}\cdot\text{m}^{-2}$ has been determined by shifting a single proton through the trap and measuring its cyclotron frequency. B_2 is 3.8 times larger than that used in a competing experiment [19] and is the highest magnetic field inhomogeneity ever superimposed to a Penning trap.

Both traps are connected by transport electrodes. The inner radius reduces along these electrodes to match the different trap radii, as shown in Fig 1. Voltage ramps are applied to the electrodes of the transport section to move the proton adiabatically between both Penning traps. The whole electrode stack is mounted in a sealed vacuum chamber and cooled to 3.8 K with a pulse tube cooler. Due to cryo-pumping the background pressure in such systems is $< 10^{-14} \text{ Pa}$. We can store a proton in our trap for arbitrarily long times (months).

Protons are produced in the precision trap by electron bombardment of a polyethylene-target and subsequent electron impact ionization. Impurity ions are selectively heated out of the trap using broadband noise and resonant radio frequency (rf) drives. Particles are then removed from the clean proton cloud until just one single particle remains. The trapped proton oscillates at three different eigenmotions [20], the modified cyclotron motion at $\nu_{+,PT} \approx 28.97 \text{ MHz}$, the axial motion at $\nu_z \approx 674 \text{ kHz}$, and the magnetron motion at $\nu_{-,PT} \approx 8 \text{ kHz}$. The oscillation of the particle induces image currents in the trap electrodes which are detected as rf voltages across a resistance R . In practice a coil is used instead of a resistor. The inductance together with the stray capacitance of the trap system forms a parallel tuned circuit with a quality factor Q . The axial frequency of the stored proton in the precision trap and in the analysis trap is measured with a superconducting Nb/Ti coil connected to both traps. The quality factor is 5800 and the effective on-resonance resistance is $36 \text{ M}\Omega$ [21]. The detection system for the measurement of the modified cyclotron frequency in the precision trap (not shown in Fig. 1) is made out of copper. It has a quality factor of 1250 and an on-resonance resistance of $380 \text{ k}\Omega$. The voltage signals induced by the proton are amplified with cryogenic low-noise amplifiers and analyzed with an FFT spectrum analyzer. The magnetron frequency is measured by side-band coupling [22] to the axial eigenmotion. The proton

interacts with the tank circuits and thus cools resistively to ambient cryogenic temperatures. The magnetic field in the center of the analysis trap is 1.17 T due to the field distortion by the ferromagnetic ring electrode. The cyclotron frequency of the proton is measured as described in [16] and is $\nu_{+,AT} \approx 17.91 \text{ MHz}$. The magnetron frequency in the analysis trap is $\nu_{-,AT} \approx 13 \text{ kHz}$.

In an ideal Penning trap the axial frequency ν_z of a trapped proton is

$$\nu_{z,0} = \frac{1}{2\pi} \sqrt{\frac{e}{m_p} \frac{d}{dz} (-\vec{\nabla} \Phi_E | \vec{e}_z)} = \frac{1}{2\pi} \sqrt{\frac{eV_0}{m_p d^2}} , \quad (2)$$

where d is a characteristic length of the trap, V_0 is the trapping voltage and $e\Phi_E$ is the electrostatic energy. In the analysis trap with its strong magnetic bottle the magnetostatic energy $\Phi_M = -\vec{\mu} \cdot \vec{B}$ contributes to the axial frequency. Here $\vec{\mu}$ is the sum of the Landau-magnetic moment which is due to the angular momentum of the cyclotron and the magnetron motion, respectively, and the magnetic moment of the proton spin $\mu_s = (g_p e \hbar m_s)/(2m_p)$, where m_s is the spin quantum number. The energy Φ_M contains a term proportional to z^2 where z is the axial distance to the center of the trap. The axial frequency thus becomes $\nu_z = \nu_{z,0} + \Delta\nu_z(n_+, n_-, m_s)$, where n_\pm denotes the number of quanta in the radial modes, and

$$\Delta\nu_z(n_+, n_-, m_s) = \frac{\hbar \nu_+}{4\pi^2 m_p \nu_z} \frac{B_2}{B_0} \cdot \left(n_+ + \frac{1}{2} + \frac{\nu_-}{\nu_+} \left(n_- + \frac{1}{2} \right) + \frac{g_p m_s}{2} \right) 3$$

A cyclotron quantum jump $\Delta n_+ = \pm 1$ corresponds to a radial energy change of $\Delta E_+ = \pm 74 \text{ neV}$ and causes an axial frequency shift of $\Delta\nu_z = \pm 68 \text{ mHz}$. A change of the magnetron quantum number leads to $\Delta\nu_z = \pm 49 \text{ }\mu\text{Hz}$. A spin-flip transition $\Delta m_s = \pm 1$ causes a jump of the axial frequency $\Delta\nu_{z,SF} = \pm 190 \text{ mHz}$. This is most important because the axial frequency can thus be used to detect the spin direction of the proton.

Spin-flip transitions are driven using a disc coil mounted close to the electrode stack as shown in Fig. 1. The coil generates a transverse magnetic rf-field \vec{b}_{rf} with frequency ν_{rf} . To drive spin flips \vec{b}_{rf} is tuned near to the Larmor frequency $\nu_L = g_p \nu_c/2$. The field penetrates into the trap through slits between the electrodes. This rf field causes a precession of the proton spin around the \vec{b}_{rf} -axis at the Rabi frequency $\Omega_R/2\pi = \nu_L b_{\text{rf}}/B_0$. In the presence of a strong magnetic bottle B_2 the spin-flip probability is given by [23]

$$P_{\text{SF}} = \frac{1}{2} \left(1 - \exp \left(-\frac{1}{2} \Omega_R^2 t_0 \chi(2\pi\nu_{\text{rf}}, B_2, T_z) \right) \right) , \quad (4)$$

where t_0 is the irradiation time, $\chi(2\pi\nu_{\text{rf}}, B_2, T_z)$ the transition lineshape and T_z the axial temperature.

The axial frequency ν_z has a strong dependence on the radial energy $E_\rho = |E_+| + |E_-|$ with $(\Delta\nu_z)/(\Delta E_\rho) \approx$

0.92 Hz/ μeV , where $|E_{\pm}|$ is the energy of the cyclotron mode and the magnetron mode, respectively. It is thus essential to avoid induced spurious changes of the radial energy of the proton. Care is taken to shield the apparatus from perturbing rf-signals and noise. In the lines for the spin-flip drive a chain of band-pass filters attenuates spurious rf-fields at the cyclotron frequency by 100 dB. The line is shorted to ground with an rf-relay whenever possible.

The frequency ν_z is measured by observing the ther-

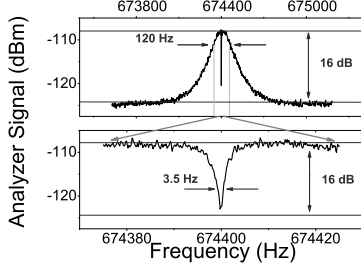


FIG. 2. Spectrum of the axial detector. The peak in the upper graph is the thermal noise spectrum of the cryogenic tank circuit. Its width is $\nu_z/Q \approx 120$ Hz. The frequency axis is stretched in the lower graph to show the narrow dip which is due to the trapped proton shorting the noise of the detector.

mal noise spectrum of the cryogenic axial tank circuit, see Fig. 2. The particle acts like a series tuned circuit, shorting the thermal noise $e_{\text{th}} = \sqrt{4k_B T_z R \Delta F}$ of the detector, where ΔF is the FFT spectrum analyzer bandwidth. The linewidth of the dip is $1/(2\pi\tau_z)$, where $\tau_z = (m_p/R) \cdot (D^2/q^2)$ is the cooling time constant and D is a characteristic length of the trap. In the precision trap the signal linewidth is 1.25 Hz and in the analysis trap 3.5 Hz due to the smaller trap-size. The detection system has a signal-to-noise ratio of 16 dB.

To determine the spin direction of the proton, the axial frequency ν_z has to be measured with high resolution. The axial frequency resolution achieved by noise-dip detection increases with measuring time Δt due to spectrum analyzer averaging. On the other hand, tiny perturbing effects can drive the radial modes and cause small changes of the axial frequency which increase with time. It was found in a series of experiments that fluctuations of the cyclotron energy at an average rate of 0.045 quantum jumps per second are responsible for the residual instability of the axial motion. Details of these experiments will be discussed in a forthcoming publication.

For the further discussion the axial frequency between time t and $t + \Delta t$ is considered and the standard deviation of $\alpha = \nu_z(t) - \nu_z(t + \Delta t)$ is defined as frequency fluctuation $\Xi = ((N-1)^{-1} \sum (\alpha_i - \bar{\alpha})^2)^{1/2}$. In our experiment at an FFT averaging time of $\Delta t_{\text{opt}} = 80$ s the frequency fluctuation is minimal, $\Xi_{\text{min}} \approx 150$ mHz. This

value is not yet sufficiently stable to detect spin flips directly in one measurement sequence as described in [24]. However, averaging can be used to detect proton spin flips.

For such a statistical measurement the axial frequency ν_z is determined in sequences of three measurements $\nu_{z,1}$, $\nu_{z,2}$, and $\nu_{z,3}$. Between the first and the second measurement a spin-flip drive is turned on near the Larmor frequency $\nu_L \approx \nu_{\text{rf}} = 50.102$ MHz. Between the second and the third measurement the rf-synthesizer is tuned to a reference frequency 100 kHz below ν_L which corresponds to approximately two linewidths. Between the third measurement and the first measurement of the following cycle $\nu_{z,1'}$ no rf-signal is applied to the trap. This sequence is repeated several hundred times and the fluctuations $\Xi_{\text{SF}} = \nu_{z,2} - \nu_{z,1}$, $\Xi_{\text{ref}} = \nu_{z,3} - \nu_{z,2}$ and $\Xi_{\text{back}} = \nu_{z,1'} - \nu_{z,3}$ are computed. If spin flips are driven the corresponding axial frequency shifts add up in a statistical way. If the spin of the proton flips in M cycles out of N , the total fluctuation is

$$\Xi_{\text{SF}} = \sqrt{\sum_i^M \frac{(\alpha_i \pm \Delta\nu_{z,\text{SF}} - \bar{\alpha})^2}{N-1} + \sum_{i=M}^N \frac{(\alpha_i - \bar{\alpha})^2}{N-1}} \approx \sqrt{\Xi_{\text{back}}^2 + P_{\text{SF}} \Delta\nu_{z,\text{SF}}^2}, \quad (5)$$

where P_{SF} is given by Eq.(4). The comparison of Ξ_{ref} and Ξ_{back} is a means to test for spurious heating of the cyclotron motion due to rf-synthesizer noise which might increase the axial frequency fluctuation. If both quantities are the same within error bars this indicates that the cyclotron motion is not affected and that an increase of Ξ is due to proton spin flips. A resolution limit for the detection of spin flips by this method is reached if the error $\sigma_{\Delta\Xi} = ((\Xi_{\text{ref}}/\sqrt{2N-2})^2 + (\Xi_{\text{SF}}/\sqrt{2N-2})^2)^{0.5}$ is of the same size as the frequency shift $\Delta\Xi = \Xi_{\text{SF}} - \Xi_{\text{ref}}$. With the conditions of our experiment for $P_{\text{SF}} = 50\%$ $\Delta\Xi = 52$ mHz are expected. This shows that it is possible to statistically detect spin flips in a series of only fifty measurement cycles.

In the experiment the measurement sequence is repeated several hundred times and the frequency fluctuations Ξ_{SF} and Ξ_{ref} are determined. The evolution of both quantities as a function of measurement cycles is shown in Fig. 3 a.) along with a confidence band given by $\sigma_{\Delta\Xi}$. Obviously, both fluctuations converge for large measuring times to nearly constant values. A significant shift of $\Delta\Xi = 47$ mHz between the reference measurement Ξ_{ref} and the resonant measurement Ξ_{SF} is observed. This means that spin flips are detected in the experiment. Using Eq. (5) we find that the average spin-flip probability is $P_{\text{SF}} = 47 \pm 7\%$. The data set has also been analyzed in a different way. The whole sequence of 800 data points is split into subsequences of 50 measurements. For every subsequence Ξ_{SF} and Ξ_{ref} are determined and binned into histograms. Figure 3 b.) shows a distinct splitting be-

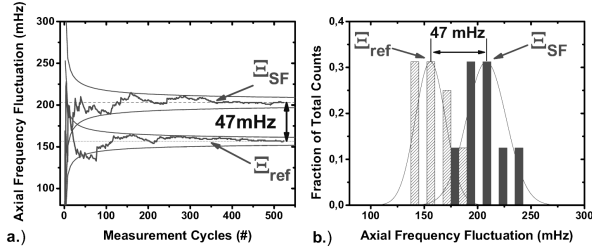


FIG. 3. Proton spin flip data. In a.) the evolution of the frequency fluctuations Ξ_{SF} and Ξ_{ref} as a function of measurement cycles is shown. The clear separation of the two lines shows that spin flips are detected. An alternative analysis is shown in b.). The entire data sequence was split into subsets and the values of Ξ_{SF} and Ξ_{ref} were binned to two histograms.

tween both distributions. This clearly shows, again, that proton spin flips are detected.

A spin flip resonance of the proton in the analysis trap has been measured by tuning ν_{rf} in steps across the Larmor frequency ν_L . For every frequency point the data are analyzed as above and the corresponding spin-flip probability P_{SF} is determined. In the magnetic bottle the Larmor frequency ν_L is a function of the particle position z . Due to the axial oscillation $z(t)$ the spin-flip resonance curve has a broad width. It is asymmetric due to the Boltzmann distribution of the axial energy. Figure 4 presents the spin-flip resonance. The solid line is the best fit of Eq. (4) to the data. Fixed parameters are the irradiation time $t_0 = 10$ s and the axial temperature of $T_z = 9.5$ K, which has been measured independently. Free fit parameters are the amplitude b_{rf} of the magnetic rf-field which comes out as $2.5 \mu\text{T}$, and the Larmor frequency ν_L . From the fit the Larmor frequency can be determined with a precision of $2 \cdot 10^{-4}$. The result is consistent with the independent measurement of the magnetic field in the analysis trap using the proton's cyclotron frequency. Figure 4 thus demonstrates, again, that proton spin flips were detected.

In the future we plan to drive the spin flip in the preci-

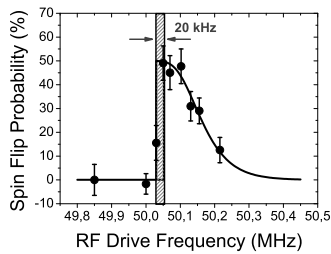


FIG. 4. Proton spin flip resonance in the analysis trap with its inhomogeneous magnetic field.

sion trap and to transport the particle into the analysis trap to analyze its spin direction [24]. In the precision trap the magnetic field is four orders of magnitude more

homogeneous than in the analysis trap and a narrow spin-flip resonance is expected. Together with a measurement of the cyclotron frequency this will be a direct high-precision measurement of the g -factor of the proton. In conclusion, spin flips of a single trapped proton have been observed for the first time. A strong magnetic bottle B_2 has been used to couple the proton spin to its axial motion in a Penning trap. The observation of tiny changes of the axial frequency clearly indicates proton spin flips. A Larmor resonance was clearly observed by averaging. This is an important break-through towards a direct precision measurement of the magnetic moment of the proton, the antiproton, and other light nuclei.

We acknowledge the support of the BMBF, the DFG (QU-122-3), the Helmholtz-Gemeinschaft, HGS-HIRE, the Max-Planck Society, Al β an (E06D101305BR) and the IMPRS-QD.

-
- [1] S. D. Bass, Rev. Mod. Phys. **77**, 1257 (2005).
 - [2] Th. Udem, A. Huber, B. Gross, J. Reichert, M. Prevedelli, M. Weitz, and T. W. Hänsch, Phys. Rev. Lett. **79**, 2646 (1997).
 - [3] S. J. Brodsky, C. E. Carlson, J. R. Hiller, and D. S. Hwang, Phys. Rev. Lett. **94**, 022001 (2005).
 - [4] R. Pohl *et al.*, Nature **466**, 213 (2010).
 - [5] S. G. Karshenboim and V. G. Ivanov, Phys. Lett. B **566**, 27 (2003).
 - [6] P. F. Winkler, D. Kleppner, T. Myint, and F. G. Walther, Phys. Rev. A **5**, 83 (1972).
 - [7] N. F. Ramsey, in: *Quantum Electrodynamics*, edited by T. Kinoshita (World Scientific, Singapore 1990), p. 673.
 - [8] C. Rodegheri, K. Blaum, H. Kracke, S. Kreim, A. Mooser, C. Mrozik, W. Quint, S. Ulmer, and J. Walz, Hyperfine Interact. **194**, 93 (2009).
 - [9] K. Blaum *et al.*, J. Phys. B: At. Mol. Opt. Phys. **42**, 154021 (2009).
 - [10] T. Pask *et al.*, J. Phys. B **41**, 081008 (2008).
 - [11] W. Quint and G. Gabrielse, Hyperfine Interact. **76**, 379 (1993).
 - [12] R. Bluhm, V. A. Kostelecky, and N. Russell, Phys. Rev. D **57**, 3932 (1998).
 - [13] H. Dehmelt and P. Ekstrom, Bull. Am. Phys. Soc. **18**, 72 (1973).
 - [14] D. Hanneke, S. Fogwell, and G. Gabrielse, Phys. Rev. Lett. **100**, 120801 (2008).
 - [15] R. S. Van Dyck, Jr., P. B. Schwinberg and H. G. Dehmelt, Phys. Rev. Lett. **59**, 26 (1987).
 - [16] N. Hermanspahn, H. Häffner, H. J. Kluge, W. Quint, S. Stahl, J. Verdu, and G. Werth, Phys. Rev. Lett. **84**, 427 (2000).
 - [17] J. Verdu, S. Djekic, H. Häffner, S. Stahl, T. Valenzuela, M. Vogel, G. Werth, H. J. Kluge, and W. Quint, Phys. Rev. Lett. **92**, 093002 (2004).
 - [18] G. Gabrielse, L. Haarsma, and S. L. Rolston, Int. J. Mass Spec. **88**, 319 (1989).
 - [19] N. Guise, J. DiSciaccia, and G. Gabrielse, Phys. Rev. Lett. **104**, 143001 (2010).
 - [20] L.S. Brown and G. Gabrielse, Rev. Mod. Phys. **58**, 233

- (1986).
- [21] S. Ulmer, H. Kracke, K. Blaum, S. Kreim, A. Mooser, W. Quint, C. C. Rodegheri, and J. Walz, Rev. Sci. Inst. **80**, 123302 (2009).
- [22] E. A. Cornell, R. M. Weisskoff, K. R. Boyce, and D. E. Pritchard, Phys. Rev. A, **41**, 312 (1990).
- [23] L. S. Brown, Ann. Phys. **159**, 62 (1985)
- [24] H. Häffner, T. Beier, N. Hermanspahn, H. J. Kluge, W. Quint, S. Stahl, J. Verdu, and G. Werth, Phys. Rev. Lett. **85**, 5308 (2000).